

Nanohybrid materials from the intercalation of imidazolium ionic liquids in kaolinite

Sadok Letaief and Christian Detellier*

Received 20th November 2006, Accepted 20th December 2006

First published as an Advance Article on the web 18th January 2007

DOI: 10.1039/b616922h

A series of novel organic–inorganic nanohybrid materials were obtained by the intercalation in the interlamellar spaces of the clay mineral kaolinite, of ionic liquids based on imidazolium derivatives. The intercalation procedure was successfully accomplished *via* a melt reaction strategy using the dimethylsulfoxide–kaolinite intercalate (DMSO-K) as a precursor. ¹³C MAS NMR as well as XRD, TGA/DTA and FTIR studies confirmed the complete displacement of DMSO molecules by the imidazolium salts during the intercalation process. Increase of the basal spacing from 1.1 nm in DMSO-K to 1.3–1.7 nm in the nanohybrid materials was observed, indicating that imidazolium derivatives are oriented in a way such that the imidazole ring is parallel, or slightly tilted by an angle of 10–25°, with respect to the kaolinite internal surfaces. The number of moles of organic material loaded in the nanohybrids was obtained from several independent measurements. The intercalation of the imidazolium salts increases the thermal stability of the resulting material by more than 150 °C with respect to DMSO-K. After heating under air at 300 °C for two hours, XRD showed that the structure of the intercalates was kept with only a slight decrease of the intercalation ratio. The original kaolinite structure was recovered after heating the intercalate at 350 °C for an additional two hours. This observed high thermal stability is promising for the use of these nanohybrid materials as precursor for the synthesis of new nanocomposites by incorporation of polymer in kaolinite at high temperature.

Introduction

Nanohybrid materials, combining organic and inorganic units at the molecular level, open the way to a large range of new functional materials. Among the choices offered for the inorganic units, clay minerals play a particularly important role.¹ The layered structuration of most of the phyllosilicates can be used as a host for the intercalation of organic guests, organised in a confined two-dimensional phase.² This intercalation is the first step towards the complete delamination of the layers in an organic polymeric matrix, leading to the formation of nanocomposite materials.^{3–6} Due to their swelling properties, smectites constitute, by far, the most used class of phyllosilicates for the preparation of nanocomposites.^{3–6}

Kaolinite is an abundant clay mineral, and is widely available. It is a 1 : 1 phyllosilicate, characterized by a dioctahedral structure, with the chemical composition Al₂Si₂O₅(OH)₄.⁷ The structural asymmetry of kaolinite, due to the superposition of the tetrahedral and octahedral sheets in the 1 : 1 layer, creates large superposed dipoles, which, in conjunction with H-bonds between the siloxane macrorings on one side and the aluminol surface on the other side, result in a large cohesive energy of the mineral.⁷ Consequently, the intercalation of molecular guests in the interlamellar spaces of kaolinite is much less developed than in the case of the smectites.^{8,9} However, kaolinite pre-intercalated with dipolar molecules, such as

DMSO, *N*-methylformamide (NMF) or urea has been used successfully as a precursor for further intercalations of other organic molecules,⁸ or of polymers.^{10–14} The intercalation can lead also to the chemical grafting of organic units on the interlamellar aluminol surfaces.^{15–22} Recently, the delamination of kaolinite was considerably promoted from such grafted derivatives.²³

Ionic liquids based on organic cations generally have a melting point below 100 °C, and some of them are liquid even at ambient temperatures. They are generally composed of a relatively bulky organic cation, such as imidazolium or pyridinium, associated with a halide anion. Their physico-chemical properties depend on the structure of the ions and can be adjusted by changing the counter-ion. They are attractive solvents as they are non-volatile, non-flammable, have a high thermal stability and are relatively inexpensive to manufacture. They are currently receiving considerable attention as a new alternative reaction medium for chemical and biocatalytic reactions, and qualify as “green solvents”.^{24–26}

The intercalation of alkylimidazolium salts in smectites, with improved thermal stability compared to the corresponding alkylammonium intercalates, was used to prepare exfoliated polyamide nanocomposites.²⁷ However, there is no report on the intercalation of alkylimidazolium salts in kaolinite. Recently, the intercalation of the ionic liquid ethylpyridinium chloride inside the interlamellar spaces of kaolinite was reported, using the melt intercalation process.^{28,29}

The intercalation of imidazolium ionic liquids in the interlamellar spaces of kaolinite was successful in the cases of the derivatives Im-*n* (*n* = 1–7) (see Fig. 1). The resulting

Centre for Catalysis Research and Innovation and Department of Chemistry, University of Ottawa, 10 Marie Curie, Ottawa, Ontario, Canada K1N 6N5. E-mail: dete@uottawa.ca

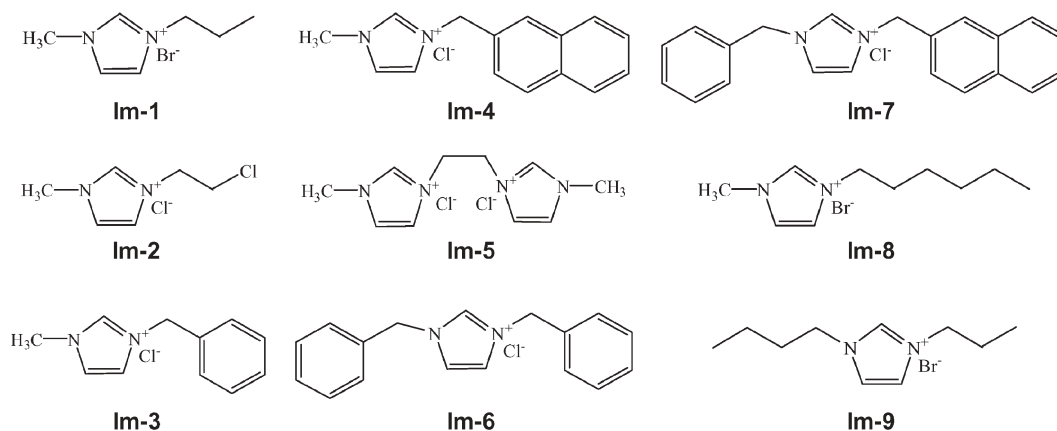


Fig. 1 Chemical structures of the ionic liquids used in the preparation of the nano hybrid materials derived from kaolinite.

alkylimidazolium intercalates are characterized by an increased thermal stability compared to most other intercalates, typically above 300 °C. These nanostructured materials constitute a promising new class of kaolinite derivatives for advanced functional applications of this abundant mineral.

Experimental

Materials

Well-crystallized kaolinite (KGa-1b; Georgia) was obtained from the Source Clays Repository of the Clay Minerals Society, Purdue University, West Lafayette, IN, USA. The purification of KGa-1b and the preparation of the dimethylsulfoxide-kaolinite intercalate (DMSO-K) were done according to previously published procedures.^{28,29} All the ionic liquids were synthesized using variations of published procedures,^{30–32} with the exception of Im-8 which was purchased from Acros Organics. Im-1, Im-2, Im-8, Im-9 are liquids at room temperature, whereas Im-3, Im-4, Im-5, Im-6 and Im-7 are solids. Their melting points are 33, 36, 74, 38 and 49 °C respectively. Imidazole, 1-methylimidazole, 1-butylimidazole, benzyl chloride and naphthyl chloride were purchased from Aldrich Chemicals and were used as received.

Synthesis and characterization of the ionic liquids

Im-1. 1-Bromopropane (12.2 mL, 133 mmol) was added dropwise to 10 g of 1-methylimidazole (122 mmol). The mixture was first stirred at room temperature for 20 minutes then at 80 °C for 48 hours under N₂. The excess of 1-bromopropane was removed by washing with diethyl ether. ¹H NMR: δ 0.21 (t, 3 H, CH₃CH₂-); 1.26 (m, 2 H, -CH₂CH₃); 3.39 (s, 3 H, CH₃-N), 3.61 (t, 2 H, -CH₂-N); 7.10–7.12 (m, 2 H, imidazole ring); 9.39 ppm (s, H, imidazole ring N-CH-N). ¹³C NMR: δ 10.1 (CH₃CH₂-); 23.0 (-CH₂CH₃); 36.0 (CH₃-N), 50.6 (-CH₂-N); 122.0 and 123.2 (imidazole ring C-C-N); 136.0 (imidazole ring N-C-N). Elemental analysis (CHN) calculated (found) for Im-1: C: 41.00% (40.59%); H: 6.35% (7.47%); N: 13.70% (13.75%).

Im-2 and Im-5. Dichloroethane (50 mL) was added to 10 g of 1-methylimidazole (122 mmol). The mixture was refluxed

overnight at 70 °C under N₂. The excess of dichloroethane was removed by evaporation. 1-Methylimidazole (2.5 g, 30 mmol) was added to 5 g of the product obtained (Im-2) (28 mmol). The mixture was stirred for 20 minutes at room temperature then at 70 °C under N₂ for 72 hours. The excess of 1-methylimidazole was removed by washing with ether. ¹H NMR: δ 3.87 (s, 6 H, CH₃-N); 4.82 (s, 4 H, -CH₂-N); 7.78 and 7.84 (s, 4 H, imidazole ring C-CH-N); 9.49 (s, 2 H, imidazole ring N-CH-N). ¹³C NMR: δ 36.7 (CH₃-N); 49.1 (-CH₂-N); 122.7 and 124.5 (imidazole ring C-C-N); 137.2 (imidazole ring N-C-N). Elemental analysis (CHN) calculated (found) for Im-5: C: 45.62% (42.17%); H: 6.08% (6.85%); N: 21.30% (19.57%).

Im-3. Benzyl chloride (15.4 mL, 133 mmol) was added dropwise to 10 g of 1-methylimidazole (122 mmol). The mixture was first stirred at room temperature for 20 minutes then at 80 °C for 72 hours under N₂. The excess of benzyl chloride was removed by washing with diethyl ether. ¹H NMR: δ 4.02 (s, 3 H, CH₃-N); 5.59 (s, 2 H, Phenyl-CH₂-N); 7.3–7.5 (m, 5 H, Phenyl-CH₂-N), 7.60 (t, 1 H, imidazole HC-CH-N); 7.74 (t, 1 H, imidazole ring C-CH-N); 10.46 (s, H, imidazole ring N-CH-N). ¹³C NMR: δ 36.4 (CH₃-N); 52.8 (Phenyl-CH₂-N); 122.0 and 123.9 (imidazole ring C-C-N); 128.8, 129.2 and 133.5 (Phenyl-CH₂-N); 137.1 (imidazole ring N-C-N). Elemental analysis (CHN) calculated (found) for Im-3: C: 63.3% (67.7%); H: 6.25% (6.55%); N: 13.4% (9.31%).

Im-4. 2-Chloromethyl-naphthalene (23.6 g, 133 mmol) was added dropwise, after gentle heating, to 10 g of 1-methylimidazole (122 mmol). The mixture was first stirred at room temperature for 20 minutes then at 80 °C for 72 hours under N₂. The excess of 2-chloromethyl-naphthalene was removed by washing with diethyl ether. ¹H NMR: δ 3.98 (s, 3 H, CH₃-N); 6.00 (s, 2 H, Naphthyl-CH₂-N); 7.16 (s, 1 H, imidazole ring C-CH-N); 7.34–7.88 (m, 7 H, Naphthyl-CH₂-N), 8.01 (d, 1 H, imidazole ring HC-CH-N); 10.26 (s, H, imidazole ring N-CH-N). ¹³C NMR δ 36.7 (CH₃-N); 51.1 (Naphthyl-CH₂-N); 122.8 and 123.5 (imidazole ring C-C-N); 121.7, 125.5, 126.6, 127.8, 128.4, 129.0, 130.6, 130.8 and 133.9 (Naphthyl-CH₂-N); 137.7 (imidazole ring N-C-N). Elemental analysis (CHN) calculated (found) for Im-4: C: 69.60% (68.17%); H: 5.80% (6.49%); N: 10.83% (10.19%).

Im-6 and Im-7. 1-Benzylimidazole was first prepared as a precursor. Imidazole (20 g, 294 mmol) was added to a mixture of DMSO–KOH (100 mL of DMSO, and 320 mmol of KOH). The system was stirred for 30 minutes at 80 °C. Benzyl bromide (55 g, 322 mmol) was then added and the mixture was stirred for two hours at 80 °C. 1-Benzylimidazole was extracted with dichloromethane, filtered (celite) and the volatile solvent was removed using a rotavapor.

Im-6. Benzyl chloride (3.8 mL, 33 mmol) was added to 4.75 g of 1-benzylimidazole (30 mmol). The mixture was stirred for 20 minutes at room temperature then at 80 °C for 72 hours under N₂. The excess of benzyl chloride was removed by washing with diethyl ether. ¹H NMR δ 5.54 (s, 4 H, Phenyl-CH₂-N); 7.33–7.48 (m, 10 H, Phenyl-CH₂-N and 2 H, imidazole ring C-CH-N); 11.01 (s, 1 H, imidazole ring N-CH-N). ¹³C NMR δ 53.2, (Phenyl-CH₂-N); 122.3 and 129.9 (imidazole ring C-C-N); 129.4, 129.8 and 133.5 (Phenyl-CH₂-N); 137.9 (imidazole ring N-C-N). Elemental analysis (CHN) calculated (found) for Im-6: C: 71.70% (69.65%); H: 5.98% (6.82%); N: 9.84% (9.83%).

Im-7. 2-Chloromethyl-naphthalene (7.9 g, 45 mmol) was added to 6.33 g of 1-benzylimidazole (40 mmol). The mixture was stirred for 20 minutes at room temperature then at 80 °C for 72 hours under N₂. The excess of 2-chloromethyl-naphthalene was removed by washing with diethyl ether. ¹H NMR δ 5.52 (s, 2 H, Phenyl-CH₂-N); 6.03 (s, 2 H, Naphthyl-CH₂-N); 7.00 (s, H, imidazole ring N-CH-C) 7.11 (s, H, imidazole ring N-CH-C); 7.33–8.1 (12 H, Phenyl-CH₂-N and Naphthyl-CH₂-N); 11.33 (s, 1 H, imidazole ring N-CH-N). ¹³C NMR δ 51.3 (Phenyl-CH₂-N); 53.5 (Naphthyl-CH₂-N); 121.3, 121.5, 122.7, 125.5, 126.6, 127.9, 128.1, 128.9, 129.1, 129.2, 129.4, 129.5, 130.8, 130.9, 132.8, 133.9, 138.1 (Naphthyl-CH₂-N, Phenyl-CH₂-N and imidazole ring -C-C-N-C-N). Elemental analysis (CHN) calculated (found) for Im-7: C: 75.3% (72.2%); H: 5.68% (6.60%); N: 8.37% (7.93%).

Im-9. 1-Bromopropane (12.2 mL, 133 mmol) was added dropwise to 15.1 g of 1-butylimidazole (122 mmol). The mixture was first stirred at room temperature for 20 minutes then at 80 °C for 48 hours under N₂. The excess of 1-bromopropane was removed by washing with diethyl ether. ¹H NMR: δ 0.78 (m, 6 H, CH₃CH₂-); 1.20 (m, 2 H, -CH₂-CH₂CH₃); 1.79 (m, 4 H, -CH₂-CH₂-N), 4.09 (m, 4 H, -CH₂-N); 7.4 (m, 2 H, imidazole ring); 8.73 (s, H, imidazole ring N-CH-N). ¹³C NMR: δ 10.1 (N-CH₂-CH₂-CH₃); 12.6 (N-CH₂-CH₂-CH₂-CH₃); 18.6 (N-CH₂-CH₂-CH₂-CH₃); 22.9 (N-CH₂-CH₂-CH₃); 31.1 (N-CH₂-CH₂-CH₂-CH₃); 49.3 (N-CH₂-CH₂-CH₃); 51.2 (N-CH₂-CH₂-CH₂-CH₃); 122.5 (imidazole ring C-C-N); 135.4 (imidazole ring N-C-N). Elemental analysis (CHN) calculated (found) for Im-9: C: 48.6% (47.01%); H: 7.69% (7.21%); N: 11.34% (11.80%).

Intercalation reaction

The imidazolium salts were intercalated in kaolinite by a melt intercalation method using DMSO-K as starting material. Typically, 1.6 g of the imidazolium salt were added to 400 mg

of DMSO-K (Im : DMSO-K = 4 : 1 w/w) at room temperature. The mixture was heated under a flow of nitrogen gas. The temperature was ramped up to 180 °C. During the heating, all the solid imidazolium salts became liquid and the modified clay (DMSO-K) was in suspension in the melt. The suspension was then magnetically stirred at 180 °C during two hours under a flow of nitrogen. The molten salt in excess was removed after four series of washing–centrifugation, using isopropanol. The recovered solid sample was dried at 60 °C overnight.

Characterization

X-Ray diffraction patterns (XRD) were obtained with a Philips PW 3710 instrument equipped with Ni-filtered and Cu-K α radiation ($\lambda = 0.15418$ nm) operating at 45 kV and 40 mA. X-Ray fluorescence (XRF) experiments were performed on a Philips PW 2400 fluorimeter. Differential thermal analyses (DTA) and thermal gravimetric analyses (TGA) were recorded on a SDT 2960 Simultaneous DSC-TGA instrument under N₂ flow (100 mL min⁻¹) with a heating rate of 10 °C min⁻¹. Infrared spectra were acquired on a Thermo Nicolet Nexus 670 FT-IR E.S.P. spectrometer under dry air using 128 scans with a resolution of 4 cm⁻¹. The spectra were recorded using KBr pellets. Before the recording of a spectrum, a flow of hot air was circulated in the room containing the pellet for 30 minutes to remove the water molecules adsorbed physically on the sample. The ¹H and ¹³C NMR spectra in solution were recorded on a Bruker 300 MHz spectrometer. The chemical shifts are referenced to TMS using CDCl₃ as a solvent.

Solid-state ¹³C NMR CP/MAS spectra were collected on a Bruker AVANCE 500 NMR spectrometer operating at 125.77 MHz. Approximately 50 mg of sample were packed in 4 mm O.D. zirconia rotors which were spun at the magic angle at speeds between 10 and 14 kHz. A cross polarization sequence was used employing a 75%–100% linear ramped pulse for the 2 ms contact pulse in the ¹³C channel. Proton 90° pulses of 3.25 μ s were used. Two pulse phase modulation (TPPM) proton decoupling was used during the 25 ms acquisition with 5.6 μ s pulses and an 84 kHz decoupling field. The recycle delay was 2 seconds. The spectral width was set at 80 kHz and 4 K data points were collected for each free induction decay. Data collection times ranged from 1 to 2.5 hours. The ¹³C chemical shifts were referenced to TMS at 0 ppm using the high frequency signal of adamantane at 38.4 ppm as a secondary standard. ²⁹Si CP/MAS spectra were collected on a Bruker AVANCE 500 NMR spectrometer operating at 99.35 MHz. Approximately 50 mg of sample were packed in 4 mm O.D. zirconia rotors which were spun at the magic angle at 6 kHz. A conventional cross polarization sequence was used with a 4.35 μ s proton 90° pulse, a 10 ms contact time and a 57 kHz CW proton decoupling field during a 40 ms acquisition time. The recycle delay was 2 seconds. The spectral width was set at 25641 Hz and 2 K data points were collected for each free induction decay. Data collection times ranged from 1 to 1.5 hours. The ²⁹Si chemical shifts were referenced to TMS at 0 ppm using the high frequency signal of tetrakis(trimethylsilyl)silane at -9.9 ppm as a secondary standard.

The ChemSketch program was provided by Advancement Chemistry Development Laboratories (ACD Labs).

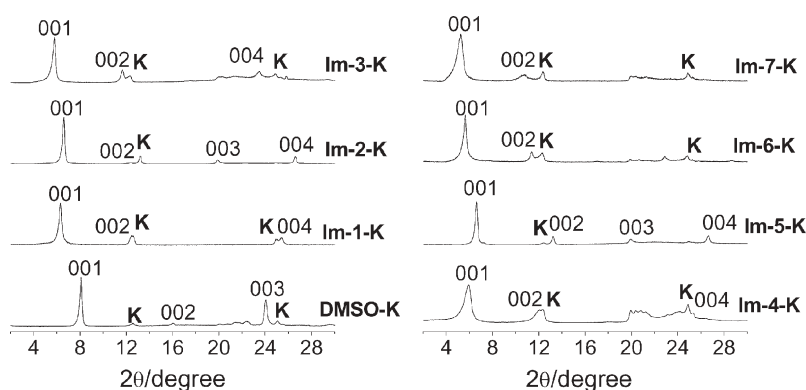


Fig. 2 Oriented XRD patterns of kaolinite intercalated with DMSO (DMSO-K) and kaolinite intercalated with imidazolium salts (Im-*n*-K, *n* = 1–7).

Results and discussion

A series of novel organic–inorganic nanohybrid materials (Im-*n*-K; *n* = 1–7) were prepared from the intercalation of a series of imidazolium salts (Fig. 1) in kaolinite pre-intercalated with dimethylsulfoxide (DMSO-K). While in the case of smectites cationic species can be easily intercalated by ion exchange with the interlamellar cation (usually sodium), the incorporation of ionic liquids into the kaolinite interlamellar spaces is more challenging due to the neutral nature of the kaolinite layers, and to the strong dipole–dipole and H-bond interactions between the octahedral and the tetrahedral sheets of adjacent layers. The intercalation occurred when DMSO-K was heated in the ionic liquid at temperatures in the range 170–180 °C, not below. In this range of temperature, DMSO was gradually removed from the kaolinite interlamellar spaces and could be replaced by the imidazolium salts. The melting point of the salt is critical in the intercalation process. If the melting point is higher than 180 °C, the intercalation can not be successful since the DMSO molecules are released before the intercalation can take place, resulting in a collapse of the structure and the recovery of the original kaolinite structure. For example, in another study in our laboratory, we have attempted to intercalate some ionic liquid derivatives from trimethylphosphine which have a melting point higher than 225 °C. The intercalation process was not successful by this approach.

The intercalation of alkyl substituted imidazolium salts was successful when the number of carbon atoms in the alkyl chain was less than 4. For longer alkyl chains, such as in the case of Im-8 and Im-9, the clay layers collapsed without insertion of the imidazolium derivatives into the interlamellar space and the original kaolinite was recovered. However, imidazolium salts substituted by aromatic groups such as benzyl and even naphthyl were successfully intercalated.

The oriented XRD patterns of the starting DMSO-K pre-intercalate as well as of the nanohybrid materials exhibit in general well developed 00*l* reflections (001, 002, 003, and 004) as shown in Fig. 2, indicating that the kaolinite layer structure is preserved after the intercalation process. In all the cases, the *d*₀₆₀ reflection of kaolinite (not shown) remains at 1.49 Å, characteristic of a dioctahedral clay mineral, showing also that the structure of the layers of kaolinite is largely unaffected by

the intercalation process. The intercalation of imidazolium salts into the interlamellar spaces of kaolinite is clearly observed by a shift of the 001 reflection to lower angles upon displacement of DMSO (*d*₀₀₁ of DMSO-K is 1.10 nm). The values of *d*₀₀₁, of Δd_{001} (obtained by subtracting the kaolinite *c*-spacing, 0.71 nm, from the observed *d*₀₀₁), of the intercalation ratio *R* (obtained as an approximation from the relative intensities of the *d*₀₀₁ peaks of the intercalate and of the non-intercalated kaolinite), and of three independent determinations of the organic content of Im-*n*-K, *n*_{TGA}, *n*_{EA}, and *n*_{thm}, obtained respectively from the TGA analysis, the elemental analysis and a structural model, are indicated in Table 1. The *d*₀₀₁ expansions (Δd_{001}) values are between 0.6 nm (Im-2; Im-5) and 1.0 nm (Im-7). They are in good agreement with those calculated using the ChemSketch program, taking into account the interatomic distances and the atomic van der Waals diameters (see below). The intercalation ratio gives an indication of the percentage of kaolinite lamellae which were submitted to intercalation. It varies in the range 78 to 98%, values expected on the basis of previous intercalation studies in kaolinite.^{15–23,33,34} The XRD peak characteristic of DMSO-K is completely removed in all the cases, indicating complete replacement by Im-*n* (*n* = 1–7) of the DMSO intercalated molecules.

The TGA–DTG traces (Fig. 3) as well as the ¹³C CP/MAS NMR spectra (Fig. 5; see below) indicate also a complete elimination of the DMSO molecules from the kaolinite

Table 1 Basal spacing (*d*₀₀₁), interlamellar expansion (Δd_{001}), intercalation ratio (*R*) and organic material content of the nanohybrid materials (number of moles of the imidazolium derivative per kaolinite structural unit Al₂Si₂O₄(OH)₄) calculated from TGA analysis, elemental analysis and a theoretical model

	<i>d</i> ₀₀₁ /nm	Δd_{001} /nm	<i>R</i> (%)	<i>n</i> _{TGA} ^a	<i>n</i> _{EA} ^b	<i>n</i> _{thm} ^c
Im-1-K	1.40	0.69	<90	0.46	0.46	0.51
Im-2-K	1.34	0.63	98	0.48	0.51	0.46
Im-3-K	1.53	0.82	89	0.48	0.58	0.40
Im-4-K	1.48	0.78	78	0.29	0.29	0.28
Im-5-K	1.34	0.63	96	0.27	0.25	0.31
Im-6-K	1.56	0.85	85	0.22	0.18	0.27
Im-7-K	1.68	0.97	84	0.22	0.20	0.22

^a Calculated from TGA analysis. ^b Calculated from elemental analysis. ^c Calculated from a theoretical model.

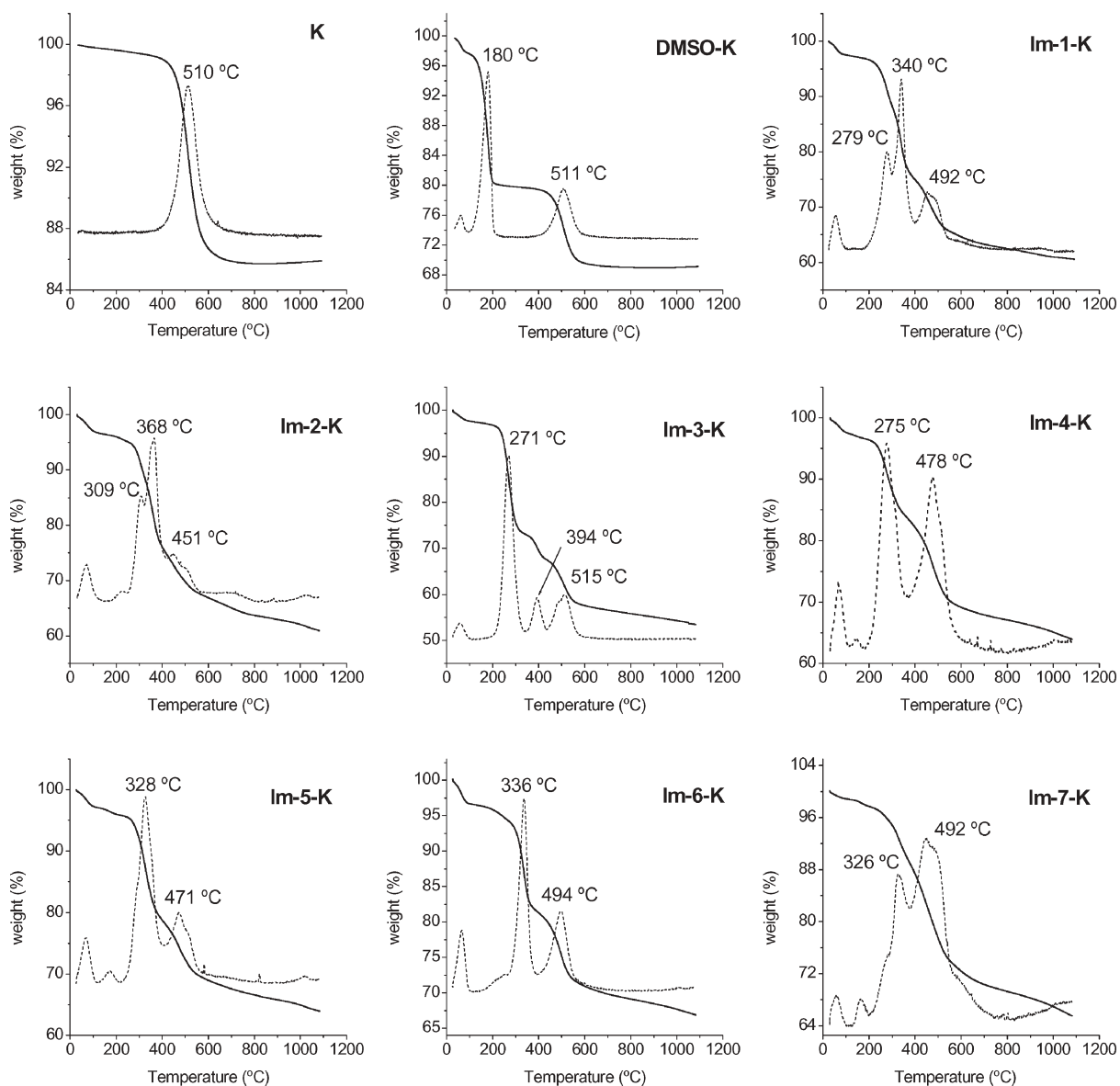


Fig. 3 TGA and DTG patterns of kaolinite (K), kaolinite intercalated with DMSO (DMSO-K), and kaolinite intercalated with imidazolium salts (Im-*n*-K; *n* = 1–7).

interlamellar spaces during the intercalation process. The TGA–DTG traces show that the imidazolium salts are removed from the kaolinite interlamellar space at maximum temperatures higher than 270 °C. Typically, a first loss is observed below 100 °C, corresponding to the removal of externally adsorbed water. Then, a second and a third losses are observed in the range of 270 °C to 350 °C and in the range of 400 °C to 515 °C. The second loss is attributed to the partial thermal removal of the organic material, while the third one is attributed to the decomposition of the remaining organic units concurrently with the kaolinite dehydroxylation. In the case of the ethylpyridinium chloride intercalate,^{28,29} the removal of the organic material was done in one step, with a maximum at 295 °C. This observed relatively high thermal stability plausibly results from the strong interactions between the imidazolium salts and the surface Al–OH (aluminol) groups through H- π interactions and between the strong ionic

interactions expected with the permanent kaolinite dipoles. In all the cases (with the exception of Im-3-K), the dehydroxylation temperature is lower than in kaolinite, as it is usually observed for intercalated kaolinite derivatives. In all the cases also, the solid-solid exothermic transformation occurred at temperatures near 1000 °C, as in the starting kaolinite.

The number of moles of organic material loaded in the nanohybrids was obtained from several experimental measurements and was compared to calculated values on the basis of the estimated volume of the salts occupying the kaolinite interlamellar spaces. Table 1 gives the number of moles of imidazolium salt per structural unit of kaolinite, $\text{Al}_2\text{Si}_2\text{O}_4(\text{OH})_4$, calculated from the TGA analysis (n_{TGA}) and from elemental analysis (n_{EA}). In some cases the amount of chlorine in the nanohybrids was determined by semi-quantitative XRF analysis. Given the large errors associated with the technique, they were in reasonable agreement with the data obtained by

TGA and elemental CHN analysis. The number of organic molecules loaded in the interlamellar spaces is smaller for the salts having the larger size, an observation in agreement with the space occupied by the organic cation along the *a,b* axes.

The molecular dimensions of the seven intercalated imidazolium salts were estimated from a space-filling structural model using the ChemSketch software from ACD labs. The volume occupied by the organic cation was approximated to a parallelepiped shape. In all the cases the molecular thickness was 0.496 nm, and the sides of the rectangular basis varied from 0.722 and 1.090 nm in the smallest case (Im-1) to 1.218 and 1.698 nm in the largest case (Im-7), corresponding to molecular parallelepiped volumes of 0.390 nm³ (Im-1) and 1.026 nm³ (Im-7). The other values fall within this range. Since the molecular thickness is close to 0.5 nm, while the *d*₀₀₁ expansions values are larger, being between 0.6 nm (Im-2; Im-5) and 1.0 nm (Im-7), the angle by which the molecule would have to be tilted to account for the observed expansion was calculated, on the basis of simple geometrical considerations. In all the cases, the values of the angle were found to be between 10 and 25 degrees. Alternatively, the observed value could result from an additional space due to the H- π interactions between the aluminol groups and the imidazolium cations lying parallel to the kaolinite layers. In any case, given the small value of the eventual calculated tilt angle, the model chosen for the calculation was based on an arrangement of the imidazolium cations parallel to the kaolinite interlamellar surfaces. The surface occupied by the salt along the *a,b* axes was then calculated by adding to the rectangular shape of the cation (for example, 0.787 nm² in the case of Im-1 and 2.068 nm² in the case of Im-7) a square shape for the anion based on its van der Waals diameter (0.144 nm² for Cl⁻). Since the surface of a unit cell of kaolinite is accepted to be typically *a* × *b* = 0.5156 nm × 0.8945 nm = 0.461 nm²,³⁵ the ratio of the unit cell surface over the surface of the imidazolium halide should give an estimate of the organic loading in Im-*n*-K. The values are also given in Table 1, as *n*_{thm}. The agreement of that value with the loading obtained from TGA analysis (*n*_{TGA}) and from elemental analysis (*n*_{EA}) is good, in support of the proposed structural model of alternating cationic and anionic species, closely packed in one layer in the kaolinite interlamellar spaces.

Fig. 4 gives the IR spectra (2600–4000 cm⁻¹ region) for kaolinite (K), the starting material (DMSO-K) and two of the intercalated materials (Im-1-K and Im-2-K). The spectra of the other nanohybrids are similar to the ones shown in Fig. 4. The spectra of kaolinite and of DMSO-K have been described previously.^{28,36} In the comparison of the spectra of Im-1-K and Im-2-K with those of kaolinite and of DMSO-K, one should particularly note two observations: the relatively sharp band observed at 3621 cm⁻¹ is still observed when the imidazolium halides have replaced DMSO. This band is attributed to the stretching vibrations of the internal hydroxyl groups. Its invariance confirms that the intercalation of imidazolium halides does not modify the 1:1 layer structure of kaolinite. The bands attributed to the stretching of the interlamellar hydroxyl groups are modified. The band at 3695 cm⁻¹ in kaolinite and DMSO-K remains observed at a close position (3697 cm⁻¹), which is in agreement with the

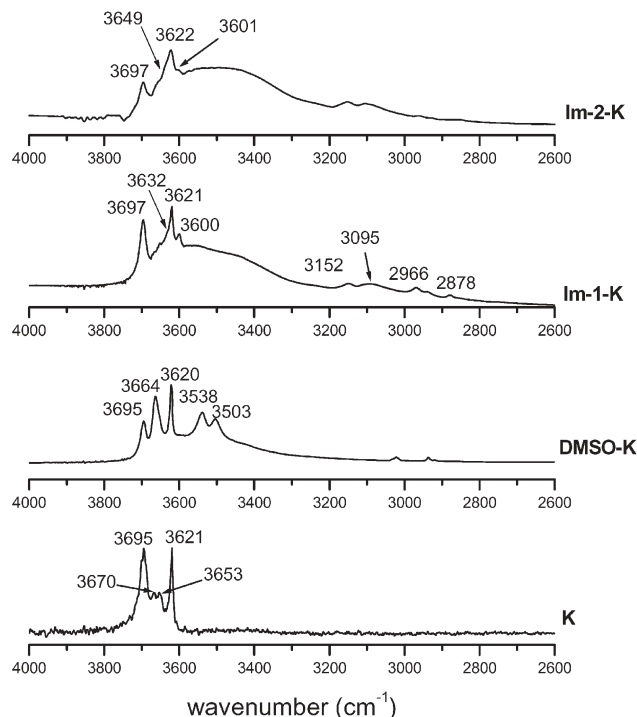


Fig. 4 IR spectra of kaolinite (K), kaolinite intercalated with DMSO (DMSO-K), and kaolinite intercalated with imidazolium salts (Im-*n*-K; *n* = 1,2).

attribution of this band to the stretching of the interlamellar hydroxyl groups pointing perpendicularly to the *c*-direction. As such, they are not directly involved in the H-bonding with organic intercalates. In strong contrast, the other bands are strongly modified by the intercalation of DMSO and of the imidazolium salts. The pattern of the IR spectra of Im-1-K and of Im-2-K in the hydroxyl stretching region, with the appearance of a new band around 3600 cm⁻¹ is similar to the patterns observed previously in the case of ethylpyridinium chloride^{28,29} or polyols^{18,19} intercalates. The broad band below 3600 cm⁻¹ is tentatively attributed to the stretching of the network of interlamellar hydroxyl groups H-bonded to the imidazolium cations.

Fig. 5 gives the ¹³C CP/MAS NMR spectra for DMSO-K and the seven Im-*n*-K intercalates. In DMSO-K, the two peaks characteristic of the unsymmetrical structuration of DMSO inside the interlamellar spaces of kaolinite are clearly observed at 43.9 and 42.8 ppm.³⁷ These peaks are totally absent from the Im-*n*-K spectra, confirming the complete removal of DMSO upon intercalation of the imidazolium salts. The ¹³C NMR spectra clearly show that the imidazolium moiety remains intact after the intercalation process. The solid-state spectra are characterized by chemical shifts close to those of the starting molecules in solution (see Experimental section). For example, the C-2 signal is systematically observed in the range 132–139 ppm, either as a well resolved peak or as a shoulder on the aromatic signals, in good agreement also with chemical shifts reported for similar compounds,³⁸ and the methyl group in position 1 is observed in the range 34–37 ppm for Im-*n*-K (*n* = 1–5). All the other signals are also in agreement with intercalated imidazolium structures corresponding to Fig. 1.

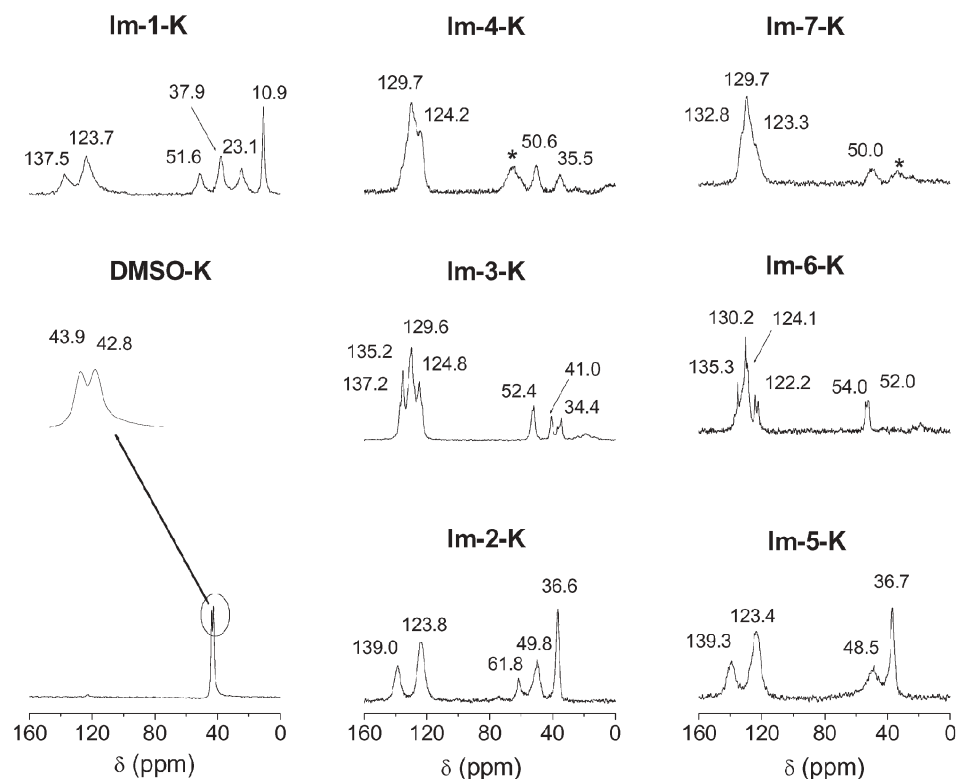


Fig. 5 Solid-state ^{13}C CP/MAS NMR spectra for the starting material (DMSO-K) and the nanohybrid materials (Im- n -K, $n = 1-7$).

The ^{29}Si CP/MAS NMR spectra of kaolinite, DMSO-K and Im- n -K ($n = 1-7$) at 99.35 MHz are shown in Fig. 6. At that frequency of observation the two signals of equal intensities characterizing kaolinite are well separated at -91.5 and -90.9 ppm.³⁹ In DMSO-K, the signal is shifted to lower frequencies, at -92.7 ppm, accounting plausibly for the keying of one of the DMSO methyl groups in the siloxane rings of the tetrahedral sheets. In contrast, the ^{29}Si NMR spectra of Im- n -K display a relatively broad envelope around -91.5 ppm, with, in some cases, finer structures. A similar spectrum was observed in the case of the ethylpyridinium chloride intercalate.^{28,29} This is an indication that the silicate layer is less affected by the presence of the imidazolium moiety than it is by the strong interactions with DMSO. This is in good agreement with a planar arrangement of the imidazolium cations in the interlamellar spaces, with no keying of the side chains in the siloxane macrorings of the tetrahedral sheets. The observation in some cases of several peaks indicates heterogeneities on the silicate surface, which is expected on the basis of the dissymmetric structures of the imidazolium derivatives. Obviously, the close interactions of phenyl, naphthyl or imidazolium rings lying parallel to the silicate surfaces lead to a distribution of dipole-induced dipole interactions, resulting in a distribution of ^{29}Si chemical shifts.

In order to evaluate further the thermal stability of these nanohybrid materials, XRD patterns were recorded after heating under air for two hours a sample of Im-1-K (Fig. 7). The intercalation ratio obtained after preparation of the sample is evaluated at 90% (the overlap of the d_{002} peak of Im-1-K with the d_{001} peak of kaolinite makes difficult a more precise determination of the intercalation ratio), with a d_{001}

value of 1.40 nm (Table 1). The TGA-DTG traces indicate a first loss of organic material at a maximum of 279 °C, followed by a second loss at 340 °C and the dehydroxylation of the kaolinite layers at 492 °C (Fig. 3). After heating at 300 °C for two hours, the XRD pattern shows that the structure of the intercalate is kept, with a d_{001} value of 1.38 nm, and an intercalation ratio of approximately 85%. This indicates that most of the imidazolium bromide units remain in the interlamellar spaces after heating at 300 °C, while a fraction of them are thermally removed. In strong contrast, after heating at 350 °C for an additional two hours, the peak at 1.38 nm disappears, and the characteristic d_{001} peak of kaolinite is obtained at 0.71 nm, showing the recovery of the original kaolinite structure. This is in agreement with the TGA-DTA analysis, giving an observed dehydroxylation temperature close to the one typically observed for kaolinite in its transformation to metakaolinite, and also with the structural reorganization of metakaolinite to mullite observed near 1000 °C⁴⁰ as would be observed for kaolinite. The thermal stability of Im-1-K is quite remarkable, particularly if compared to what was observed previously in the case of the ethylpyridinium chloride intercalate, where the organic material was completely removed at 250 °C under the same conditions.²⁸

This new class of organic-inorganic nanohybrid materials, prepared simply and easily from the dispersion of the DMSO-kaolinite intercalate in the ionic liquid at 180 °C, are characterized by well-ordered structures and show thermal stability when heated at temperatures up to 300 °C. The intercalation process can not be predicted based upon simple factors such as the molecular size of the salt or the melting point. For example, the intercalation of Im-7 was successful while that of

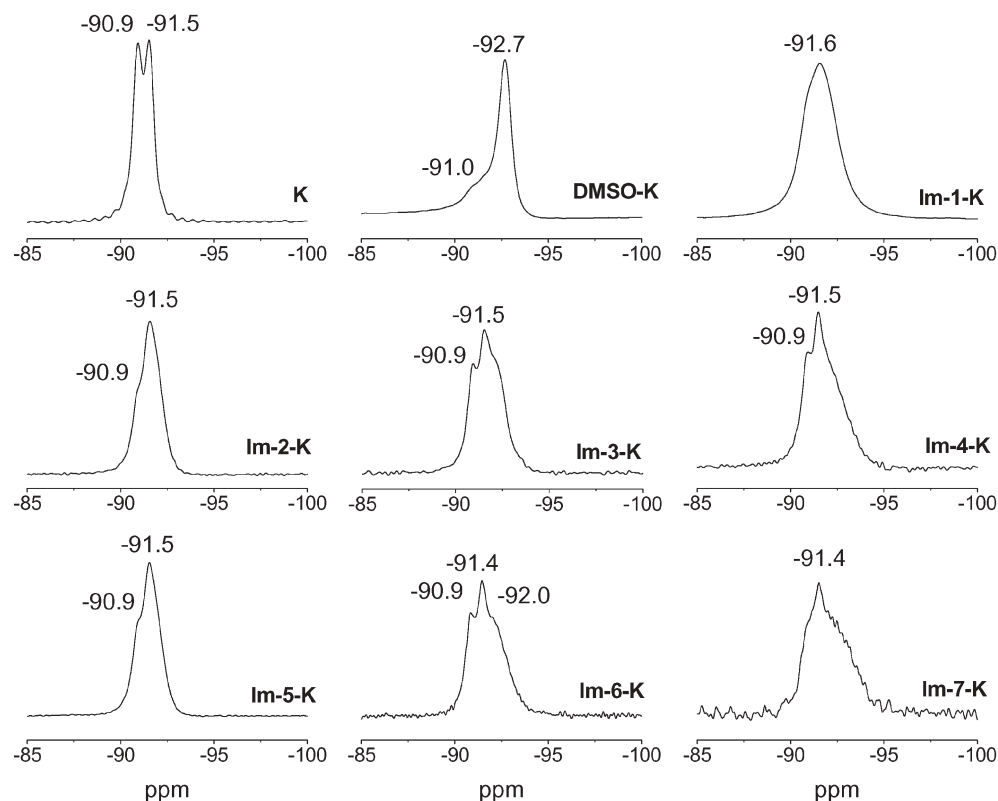


Fig. 6 Solid-state ^{29}Si spectra for kaolinite (K), the starting material (DMSO-K) and the nanohybrid materials (Im- n -K, $n = 1-7$).

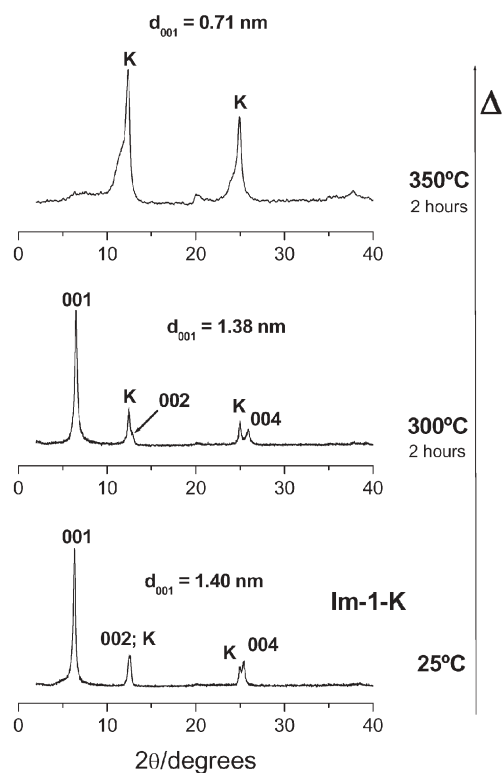


Fig. 7 XRD patterns of an oriented sample of Im-1-K at room temperature and heated successively during two hours at 300 °C and 350 °C under static air.

Im-9 was not. The former is bulkier, and solid at room temperature. The second is smaller and liquid at room temperature. A series of factors contribute to the successful intercalation, one of them being the ability of the incoming guest to replace in a concerted way the departing DMSO molecules to avoid a collapse of the structure and the recovery of kaolinite. The process occurs in a concerted manner, concurrently, not in sequence.

In summary, the reactions of imidazolium derivatives with kaolinite pre-intercalated with DMSO under melt conditions constitute an efficient route for the preparation of novel nanostructured materials which are attractive as precursors for the preparation of other nanohybrid and nanocomposite materials. The nature and the length of the alkyl chain substituting the imidazolium cation, as well as the nature of the counter-anion, are critical for the success of the intercalation process. The high thermal stability of these intercalates coupled with the electric properties of the imidazolium salts could provide improved materials with electronic conductivity behaviour. The relationship between the nanoscale organization of the organic salts in the interlamellar spaces of the clay minerals and the electric conductivity are currently under investigation in our laboratory.

Acknowledgements

This work was financially supported by a Discovery Grant of the Natural Sciences and Engineering Research Council of Canada (NSERC). Dr Raed Abu Rezk is thanked for fruitful

discussions. Dr Glenn A. Facey is thanked for recording the NMR spectra and Dr Ron Hartree for the XRF measurements.

References

- 1 *Handbook of Clay Science*, in *Developments in Clay Science, 1*, ed. F. Bergaya, B. K. G. Theng and G. Lagaly, Elsevier, Amsterdam, 2006.
- 2 E. Ruiz-Hitzky, *Organic-inorganic materials: from intercalations to devices*, in *Functional Hybrid Materials*, ed. P. Gómez-Romero and C. Sánchez, Wiley-VCH, Weinheim, 2004, ch. 2, pp. 15–49.
- 3 M. Alexandre and P. Dubois, *Mater. Sci. Eng., R.*, 2000, **28**, 1–283.
- 4 S. Sinha Ray and M. Okamoto, *Prog. Polym. Sci.*, 2003, **28**, 1539–1641.
- 5 E. Ruiz-Hitzky and A. Van Meerbeek, *Clay Mineral- and Organoclay-polymer Nanocomposite*, in *Developments in Clay Science, 1, Handbook of Clay Science*, ed. F. Bergaya, B. K. G. Theng and G. Lagaly, Elsevier, Amsterdam, 2006, ch. 10.3, pp. 583–621.
- 6 *Polymer-clay nanocomposites*, ed. T. J. Pinnavaia and G. Beall, Wiley Series in Polymer Science, Wiley, New York, 2000.
- 7 *Hydrous Phyllosilicates*, ed. S. W. Bailey, American Mineralogical Society, Washington DC, 1988.
- 8 G. Lagaly, M. Ogawa and I. Dékány, *Clay Mineral Organic Interactions*, in *Developments in Clay Science, 1, Handbook of Clay Science*, ed. F. Bergaya, B. K. G. Theng and G. Lagaly, Elsevier, Amsterdam, 2006, ch. 7.3, pp. 309–377.
- 9 R. L. Frost and J. Kristof, *Interface Sci. Technol.*, 2004, **1**, 184–215.
- 10 T. A. Elbokl and C. Detellier, *J. Phys. Chem. Solids*, 2006, **67**, 950–955.
- 11 J. J. Tunney and C. Detellier, *Chem. Mater.*, 1996, **8**, 927–935.
- 12 Y. Komori, Y. Sugahara and K. Kuroda, *Chem. Mater.*, 1999, **11**, 3–6.
- 13 T. Itagaki, Y. Komori, Y. Sugahara and K. Kuroda, *J. Mater. Chem.*, 2001, **11**, 3291–3295.
- 14 J. E. Gardolinski, L. C. M. Carrera, M. P. Cantão and F. Wypych, *J. Mater. Sci.*, 2000, **35**, 3113–3119.
- 15 J. J. Tunney and C. Detellier, *Chem. Mater.*, 1993, **5**, 747–748.
- 16 J. J. Tunney and C. Detellier, *J. Mater. Chem.*, 1996, **6**, 1679–1685.
- 17 J. J. Tunney and C. Detellier, *Clays Clay Miner.*, 1994, **42**, 552–560.
- 18 K. B. Brandt, T. A. Elbokl and C. Detellier, *J. Mater. Chem.*, 2003, **13**, 2566–2572.
- 19 T. A. Elbokl and C. Detellier, *Clay Sci.*, 2005, **12**, 38–46.
- 20 T. Itagaki and K. Kuroda, *J. Mater. Chem.*, 2003, **13**, 1064–1068.
- 21 J. Murakami, T. Itagaki and K. Kuroda, *Solid State Ionics*, 2004, 279–282.
- 22 J. E. F. C. Gardolinski and G. Lagaly, *Clay Miner.*, 2005, **40**, 537–546.
- 23 J. E. F. C. Gardolinski and G. Lagaly, *Clay Miner.*, 2005, **40**, 547–556.
- 24 M. J. Earle and K. R. Seddon, *Pure Appl. Chem.*, 2000, **72**, 1391–1398.
- 25 Z. Yang and W. Pan, *Enzyme Microb. Technol.*, 2005, **37**, 19–28.
- 26 N. Winterton, *J. Mater. Chem.*, 2006, **16**, 4281–4293.
- 27 N. Gilman, W. H. Awad, R. D. Davis, J. Shields, R. H. Harris, C. Davis, A. B. Morgan, T. E. Sutto, J. Callahan, P. C. Trulove and H. C. DeLong, *Chem. Mater.*, 2002, **14**, 3776–3785.
- 28 S. Letaief and C. Detellier, *J. Mater. Chem.*, 2005, **15**, 4734–4740.
- 29 S. Letaief, T. A. Elbokl and C. Detellier, *J. Colloid Interface Sci.*, 2006, **302**, 254–258.
- 30 E. A. Turner, C. C. Pye and R. D. Singer, *J. Phys. Chem. A*, 2003, **107**, 2277–2288.
- 31 P. B. Webb, M. F. Sellin, T. E. Kunene, S. Williamson, M. Z. S. Alexandra and D. J. Cole-Hamilton, *J. Am. Chem. Soc.*, 2003, **125**, 15577–15588.
- 32 O. V. Starikova, G. V. Dolgushin, L. I. Larina, P. E. Ushakov, T. N. Komarova and V. A. Lopyrev, *Russ. J. Org. Chem.*, 2003, **39**, 1467–1470.
- 33 J. J. Tunney and C. Detellier, *Can. J. Chem.*, 1997, **75**, 1766–1772.
- 34 Y. Deng, G. N. White and J. B. Dixon, *J. Colloid Interface Sci.*, 2002, **250**, 379–393.
- 35 R. F. Giese, Jr., *Kaolin Minerals: Structures and Stabilities*, in *Hydrous Phyllosilicates*, ed. S. W. Bailey, American Mineralogical Society, Washington DC, 1988, ch. 3, pp. 29–66.
- 36 W. N. Martens, R. L. Frost, J. Kristof and E. Horvath, *J. Phys. Chem. B*, 2002, **106**, 4162–4171.
- 37 S. Hayashi, *Clays Clay Miner.*, 1997, **45**, 724–732.
- 38 J. Alcázar, A. de la Hoz and M. Begtrup, *Magn. Reson. Chem.*, 1998, **36**, 296–299.
- 39 J. Sanz and J. M. Serratos, *J. Am. Chem. Soc.*, 1984, **106**, 4790–4793.
- 40 L. A. Pérez-Maqueda, J. L. Pérez-Rodríguez, G. W. Scheiffle, A. Justo and P. J. Sánchez-Soto, *J. Therm. Anal.*, 1993, **39**, 1055–1067.